Coronal and Chromospheric Properties of Flare-Imminent versus Flare-Quiet Active Regions

K.D. Leka[1,2], K. Dissauer[1], G. Barnes[1], E.L. Wagner[1]
[1]NorthWest Research Associates, Boulder, CO, USA
[2]Institute for Space-Earth Environmental Research, Nagoya University, Nagoya, Japan
kdleka@isee.nagoya-u.ac.jp leka@nwra.com dissauer@nwra.com graham@nwra.com wagneric@nwra.com

Introduction

Solar flare forecasting has focused on characterizing an active region's complexity using white-light images, photospheric magnetic field maps (and extrapolations using those maps as boundary conditions), and chromospheric morphology. We report on the results of a large-sample study of "AIA Active-Region Patches" (AARP) regions that uses NonParametric Discriminant Analysis through the NWRA Classification Infrastructure (NCI) to ask the question of what distinguishes flare-imminent vs. flare-quiet active regions (or epochs during a region's evolution). Parametrizing using area-summations and high-order moment analysis on both direct and running-difference images in multiple AIA wavelength bands, we find top Brier Skill Scores in the 0.07 – 0.33 range, True Skill Statistics in the 0.68 – 0.82 range (depending on event definition), and Receiver Operating Characteristic Skill Scores above 0.8. We find evidence for enhanced heating and kinematics in flare-imminent samples. Coronal- and chromospheric- targeted parameters, like the commonly-used photosphere-magnetic field parameters, are candidates for improved physics-based understanding of the flare-ready atmosphere, and improved flare forecasting.

AARP Database

AIA Active Region Patches (AARPs) [3] are region-targeted extractions of AIA full-disk data analogous to HMI Active Region Patches (HARPs) that are defined using the line-of-sight photospheric field [1]. AARPs are extracted from EUV images in 94, 131, 171, 193, 211, 304, 335 Å covering the chromosphere to corona, sensitive to emission from temperatures ranging from 0.5 to 10 MK, plus the UV 1600 Å sensitive to upper photosphere and transition region emission at 0.1 MK. Temporal downsampling consists of bursts of 13 minutes of data sampled at 72s, hourly for 7 hours centered at :48 (15:48– 21:48 UT). The AARP dataset is coordinated with data previously produced for photospheric active region investigations using the vector photospheric field [6].

Date Range	HARP Range	NOAA AR Range	# Samples	# AARP days	Archive
06/2010 – 12/2018	36 – 7331	11073 – 12731	256,976	32,067	≈ 9.5 TB

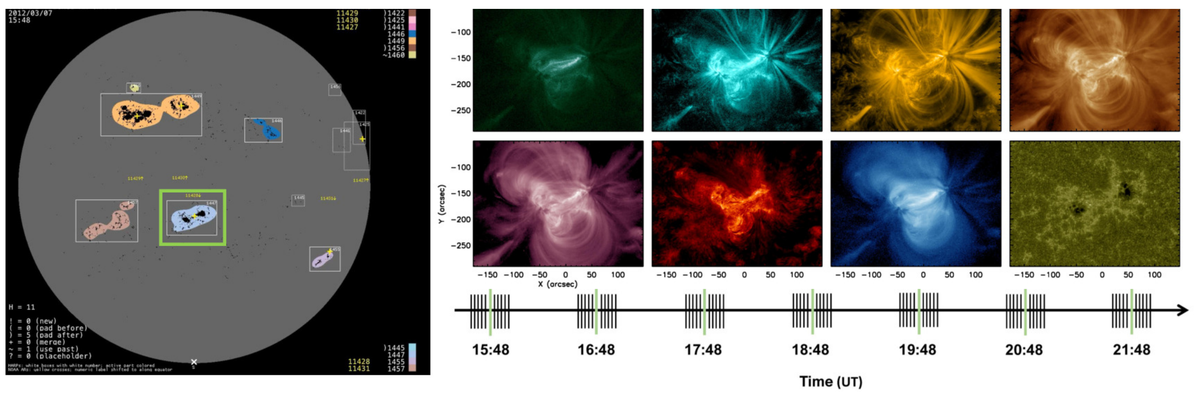

Overview of the AARP extraction and down-sampling in the spatial and temporal domains: HARP/AARP 1447 on March 07, 2012. **All AARP data (FITS files) will be available through the NASA/Solar Data Analysis Center.**

Parametrization of Chromospheric, Transition Region, and Coronal Behavior

"For solar active regions, are flare-imminent epochs distinguishable from flare-quiet epochs on the basis of chromospheric and coronal emission and kinematics?" We ask this using UV and EUV intensity images and HMI-defined active regions, *without* the benefit of spectroscopy [9], but *with* time-series analysis [2] in order to enhance physical interpretation of the results. Moment analysis, including higher-order moments, describes bulk properties and the more behavior of the distribution wings respectively. The parametrization uses the "direct" images ("I"), and the running-difference images ("ΔI"):

- The total brightness $\Sigma(\mathrm{I}_*)$, and total running-difference $\Sigma(\Delta\mathrm{I}_*)$, are extensive parameters that scale with size of the target.
- The moments of the brightness distribution $\mathcal{M}(\mathrm{I}_*)$: the mean $\mu(\mathrm{I}_*)$, standard deviation $\sigma(\mathrm{I}_*)$, skew $\varsigma(\mathrm{I}_*)$, and kurtosis $\kappa(\mathrm{I}_*)$; moments are intensive parameters that do not scale with target size. Similarly, the moments of the running-difference image distributions $\mathcal{M}(\Delta\mathrm{I}_*)$.
- For each of the 80 base parameters we derive a "static" state and its temporal behavior $d\mathrm{X}/d\mathrm{t}$, using the slope and intercept of a linear fit, for a final tally of 160 parameters evaluated.
- Note: The $\Delta\mathrm{I}_*$ parameters summarize high-frequency variation; the $d\mathrm{X}/d\mathrm{t}$ parameters summarize the longer-term trends in behavior, including that of high-frequency variations.
- These parametrizations are chosen to be physically interpretable. For example the appearance of new bright loops will enhance overall brightness levels of, *e.g.*, 171Å images ($\Sigma(\mathrm{I}_{171})$) and the mean brightness levels ($\mu(\mathrm{I}_{171})$), but also produce a positive skew in the associated running-difference images ($\varsigma(\Delta\mathrm{I}_{171})$) as the new loops appear.

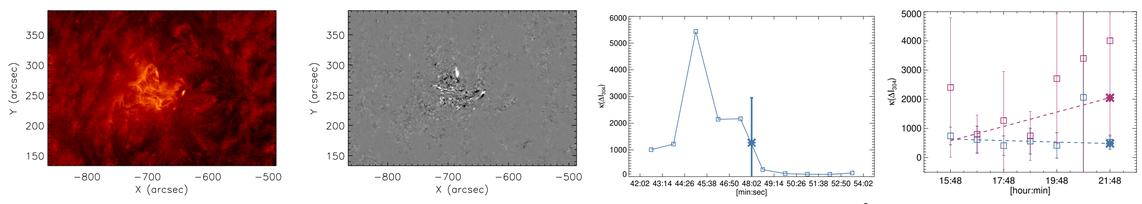

Steps for parametrizing the AARPs. The direct and running-difference images of 304Å are shown (left two panels); the kurtosis of the running-difference images is calculated for the 13min (11 images) ("$\kappa(\Delta I_{304})$", mid-right, □) from which the mean and standard deviation are shown (∗ ±); these become the data points for each of the samples covering 7 hours (right, □±), from which the linear slope and last-data (21:48 UT) intercept (∗) provide the final inputs for nonparametric discriminant analysis. Shown: a "no-event" epoch @2011.07.25 and "yes-event" epoch @2011.07.26.

NWRA Classification Infrastructure (NCI)

- Well-established statistical classifier system based on Nonparametric Discriminant Analysis (NPDA) [6].
- Four components at work in this facility: the input parameters, the event definitions and event lists, the statistical package, and the evaluation metrics.
- NPDA: functional form of the distributions is not assumed, but estimated from the data.
- *New capabilities*: adaptive kernel for density estimates, multiple population (as well as multiple parameter) discriminant analysis, region-based cross-validation.
- Bootstrap with replacement [4, 5, 6], also region-based with-holding, provides uncertainties on the evaluation metrics.

[1] M. G. Bobra, X. Sun, J. T. Hoeksema, M. Turmon, et al.: 2014 *Sol. Phys.*, **289**, 3549âĂŞ3578.
[2] T. Cinto, A. L. S. Gradvohl, G. P. Coelho, A. E. A. da Silva: 2020, *Sol. Phys.*, **295**, 93.
[3] K. Dissauer, K. D. Leka, E. L. Wagner: 2023, *Astrophys. J.*, **942**, 83.
[4] B. Efron & G. Gong: 1983, *Am. Stat.*, **37**, 36.
[5] I. T. Jolliffe & D. Stephenson,: 2012, *Forecast Verification: A Practioner's Guide in Atmospheric Science*, 2nd Edition (The Atrium, Southern Gate, Chichester, West Sussex PO19 8SQ, England: Wiley).
[6] K. D. Leka, G. Barnes, and E. L. Wagner: 2018, *Journal of Space Weather and Space Climate* **8**, 655 A25.
[7] K. D. Leka, K. Dissauer, G. Barnes, E. L. Wagner 2023:*Astrophys. J.*, **942**, 84.
[8] J. R. Lemen, A. M. Title, D. J. Akin, P. F. Boerner, et al.: 2012, *Sol. Phys.*, **275**, 17-40.
[9] B. Panos & L. Kleint, L.: 2020, *Astrophys. J.*, **891**, 17.
[10] W. D. Pesnell, B. J. Thompson, and P. C. Chamberlin: 2012 *Sol. Phys.*, **275**, 3âĂŞ15.

This work was funded primarily from NASA/GI Grant 80NSSC19K0285 with final support from NASA/GI Grant 80NSSC21K0738 and NSF/AGS-ST Grant 2154653, and preparation and publication support from Nagoya University / ISEE.

Event Definitions

Label	GOES lower limit ($10^{-6}\,\mathrm{W\,m^{-2}}$)	Validity Period (hr)	Latency Period (hr)	# Events, Event Rate
C1.0+/24 hr	1.0	24	0.2	2752 (0.086)
M1.0+/24 hr	10.0	24	0.2	450 (0.014)
C1.0+/6 hr	1.0	6	0.2	1262 (0.039)
M1.0+/6 hr	10.0	6	0.2	155 (0.005)

The Take-Away Points:

- Total emission can identify flare-ready regions, but mean brightness measures do not: *this is the well-known active-region-size/flare-productivity relation.*
- Once a region is flare productive, the active-region coronal plasma appears to stay hot.
- 94 Å provides the most parameters with discriminating power; it probably benefits from sampling multiple physical regimes.
- Flare-imminent regions preferentially display short-lived small-scale brightening events.
- Longer-term evolution and trends can provide flare-imminent information, *but at no strong preference over "static" parameters.*
- Improvements to flare forecasts will likely come by combining coronal and photospheric data.

Example NonParametric Probability Density Functions

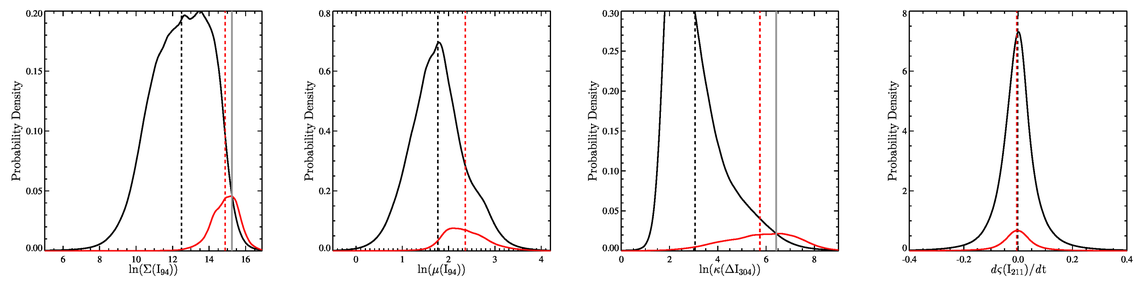

NonParametric Probability Density Functions of four parameters for the C1.0+/24 hr event definition: (left-to-right): the total of the 94Å emission ($\ln\Sigma(I_{94})$), the mean of the 94Å emission ($\ln\mu(I_{94})$), the kurtosis of the running-difference of 304Å images ($\ln\kappa(\Delta I_{304})$), and the change with time of the skew of the 211Å emission ($d\varsigma(\mathrm{I}_{211})/dt$). For all, the **event**, **non-event** non-parametric density estimates using an adaptive kernel are shown, their means (**- - -/- - -**), and the **discriminant boundary(ies)**.

Coronal & Chromospheric Indicators of Flare-imminent vs. Flare-Quiet Active Region Epochs

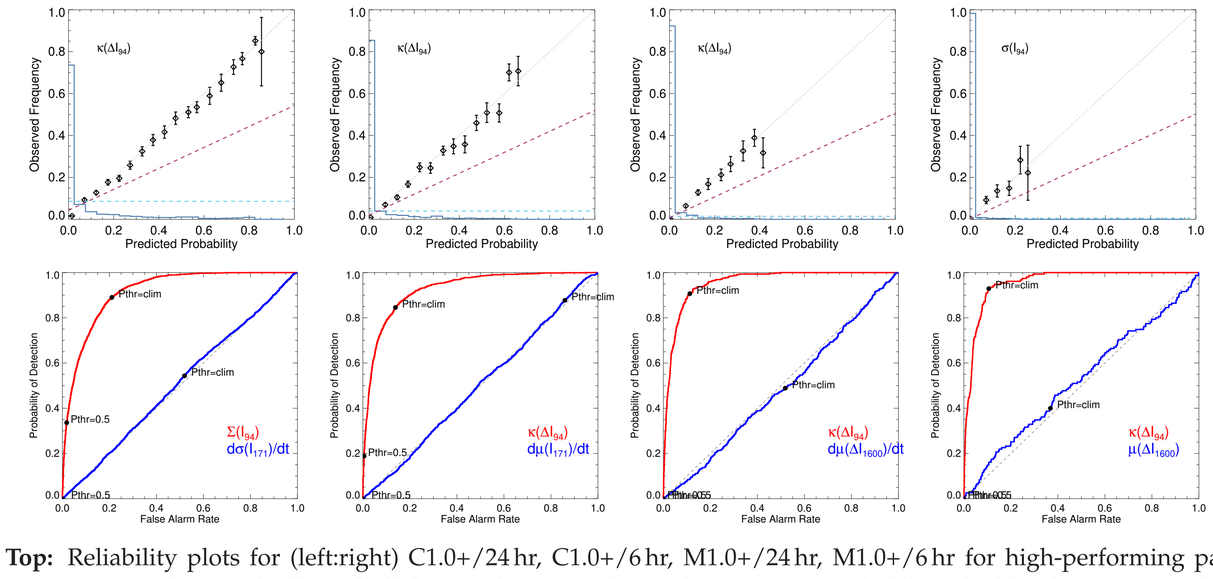

Top: Reliability plots for (left:right) C1.0+/24 hr, C1.0+/6 hr, M1.0+/24 hr, M1.0+/6 hr for high-performing parameters according to the Brier Skill Scores; the $x = y$ line indicates perfect reliability, the blue histogram is the frequency of occurrence for each prediction bin, the light-blue horizontal line indicates the climatology and the red dashes indicate the "no skill" line. Error bars reflect the sample size in each bin. **Bottom:** Receiver Operating Characteristic (ROC) plots for (left:right) C1.0+/24 hr, C1.0+/6 hr, M1.0+/24 hr, M1.0+/6 hr, for the parameters as indicated, generally in the top-10 or bottom-5 scoring group.

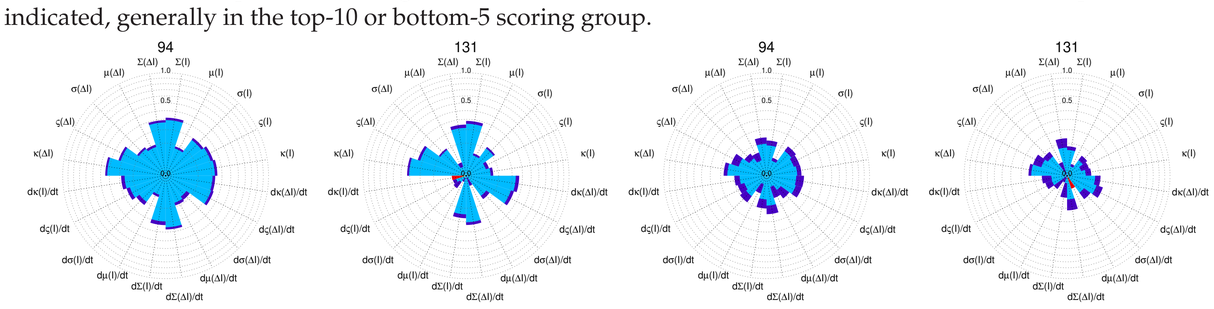

Radar plots showing Brier Skill Score for all parameters, grouped by filter, as labeled. Arcs indicate the range of the BSS $\pm\,\sigma$BSS, BSS > 0 (blue) and |BSS| for BSS < 0 (orange), with darker hues indicating the uncertainty ranges. Shown: C1.0+/24 hr event definition results for two filters 94Å and 131Å (left) and M1.0+/24 hr event definition results for the same two filters (right).

Sample Skill Scores & Metrics

Parameter	Brier Skill Score	Max(TSS)	$\mathcal{G}$ini (ROCSS)	Parameter	Brier Skill Score	Max(TSS)	$\mathcal{G}$ini (ROCSS)
Top 10 Scoring Parameters: C1.0+/24 hr				**Top 10 Scoring Parameters: M1.0+/24 hr**			
$\kappa(\Delta\mathrm{I}_{94})$	0.332 ± 0.011	0.650	0.816	$\kappa(\Delta\mathrm{I}_{94})$	0.160 ± 0.015	0.794*	0.909*
$\kappa(\Delta\mathrm{I}_{131})$	0.315 ± 0.011	0.658	0.810	$\kappa(\Delta\mathrm{I}_{131})$	0.132 ± 0.010	0.734	0.862
$\kappa(\Delta\mathrm{I}_{171})$	0.312 ± 0.012	0.670	0.809	$\Sigma(\Delta\mathrm{I}_{94})$	0.131 ± 0.015	0.704	0.840
$\kappa(\Delta\mathrm{I}_{304})$	0.310 ± 0.010	0.668	0.812	$d\kappa(\Delta\mathrm{I}_{94})/d\mathrm{t}$	0.125 ± 0.018	0.680	0.837
$\Sigma(\mathrm{I}_{94})$	0.302 ± 0.013	0.680*	0.830*	$\Sigma(\Delta I_{131})$	0.118 ± 0.021	0.640	0.786
$\kappa(\Delta\mathrm{I}_{193})$	0.301 ± 0.011	0.657	0.814	$\kappa(\Delta\mathrm{I}_{211})$	0.117 ± 0.008	0.750	0.863
$\kappa(\Delta\mathrm{I}_{211})$	0.291 ± 0.011	0.651	0.794	$d\varsigma(\Delta\mathrm{I}_{94})/d\mathrm{t}$	0.116 ± 0.009	0.640	0.802
$\Sigma(\Delta\mathrm{I}_{94})$	0.286 ± 0.011	0.626	0.788	$\kappa(\Delta\mathrm{I}_{304})$	0.116 ± 0.010	0.725	0.851
$\Sigma(\mathrm{I}_{335})$	0.280 ± 0.014	0.672	0.822	$d\varsigma(\Delta\mathrm{I}_{131})/d\mathrm{t}$	0.110 ± 0.016	0.658	0.812
$d\Sigma(\Delta I_{94})/d\mathrm{t}$	0.273 ± 0.011	0.597	0.761	$d\Sigma(\Delta\mathrm{I}_{131})/d\mathrm{t}$	0.109 ± 0.017	0.626	0.764
Bottom 5 Scoring Parameters: C1.0+/24 hr				**Bottom 5 Scoring Parameters: M1.0+/24 hr**			
$d\mu(I_{193})/d\mathrm{t}$	0.001 ± 0.000	0.035	0.046	$d\sigma(I_{171})/d\mathrm{t}$	0.000 ± 0.000	0.049	0.038
$\mu(\Delta I_{171})$	0.001 ± 0.001	0.052	0.047	$d\mu(I_{171})/d\mathrm{t}$	0.000 ± 0.000	0.028	0.019
$d\sigma(I_{171})/d\mathrm{t}$	0.000 ± 0.000	0.023	0.015	$d\mu(\Delta I_{1600})/d\mathrm{t}$	0.000 ± 0.000	-0.031*	-0.036*
$d\kappa(I_{131})/d\mathrm{t}$	-0.011 ± 0.009	0.203	0.283	$\mu(\Delta I_{1600})$	0.000 ± 0.000	-0.031	-0.024
$d\kappa(I_{335})/d\mathrm{t}$	-0.068 ± 0.028	0.160	0.262	$d\mu(I_{131})/d\mathrm{t}$	-0.002 ± 0.004	0.157	0.197

*: Top or Bottom score for Max(TSS) and for $\mathcal{G}$.
For C1.0+/24 hr the worst Max(TSS)= -0.038, and $\mathcal{G}$= -0.034 both for $d\varsigma(I_{211})/d\mathrm{t}$ which has BSS= 0.001 ± 0.001.

Interpretation and Additional Points

- *Running-Difference images dominate the top-scoring parameters.* The short-duration fluctuations or temporal changes are overall important to consider, in addition to "direct" images of the coronal & transition region.
- *The fluctuations are small.* Higher-order moments of running-difference images are most influenced by spatially small-scale but intense variations. Spatially binning the AIA images will cause these characteristics to be lost.
- *Longer-term evolution dominates in the bottom-scoring parameters.* The temporal variation of the image brightness distributions over a few hours generally do not well-separate the flare-ready samples.
- *Solar cycle makes very little difference.* Cycle-related event-rate variations are more impactful to classification success than, *e.g.* background emission variations. (Details in Leka+2023).